Title

Retinal degeneration in two lines of transgenic S334ter rats

Permalink

https://escholarship.org/uc/item/8jb105k2

Journal

Experimental Eye Research, 92(3)

ISSN

0014-4835

Authors

Martinez-Navarrete, G
Seiler, MJ
Aramant, RB
et al.

Publication Date

2011-03-01

DOI

10.1016/j.exer.2010.12.001

Retinal degeneration in two lines of transgenic *S334ter* rats

G. Martinez-Navarrete [a,1], M.J. Seiler [b,c,d,*,1], R.B. Aramant [d,e], L. Fernandez-Sanchez [a], I. Pinilla [f], N. Cuenca [a,**]

[a] Department of Physiology, Genetics, Microbiology, University of Alicante, Spain
[b] Department of Ophthalmology, University of Southern California, Los Angeles, CA, USA
[c] Department of Anatomy & Cell Biology, University of Southern California, Los Angeles, CA, USA
[d] Department of Anatomy & Neurobiology, UC Irvine, Irvine, CA, USA
[e] Department of Anatomical Sciences & Neurobiology, University of Louisville, Louisville, KY, USA
[f] Department of Ophthalmology, University Hospital Lozano Blesa, Aragones Institute of Health Science. Zaragoza, Spain

ARTICLE INFO

ABSTRACT

Aim of this study was to examine synaptic connectivity changes in the retina and the location and rate of apoptosis in transgenic *S334ter* line-3 and line-5 rats with photoreceptor degeneration. Heterozygous *S334ter*-line-3 and line-5 at P11-13, P30, P60, P90 and several control non-dystrophic rats (Long Evans and Sprague–Dawley) at P60, were studied anatomically by immunohistochemistry for various cell and synaptic markers, and by PNA and TUNEL label.- *S334ter* line-3 exhibited the fastest rate of degeneration with an early loss of photoreceptors, with 1–2 layers remaining at P30, and only cones left at P60. Line-5 had 4–5 layers left at P30, and very few rods left at P60-90. In both lines, horizontal cell processes (including dendrites and axon) were diminished at P11-13, showing gaps in the outer plexiform layer (OPL) at P60, and at P90, almost no terminal tips could be seen. Bipolar cells showed a retraction of their dendrites forming clusters along the OPL. Synaptic terminals of A-II amacrine cells in the IPL lost most of their parvalbumin-immunoreactivity. The apoptosis rate was different in both lines. Line-3 rats showed many photoreceptors affected at P11, occupying the innermost part of the outer nuclear layer. Line-5 showed a lower number of apoptotic cells within the same location at P13. In summary, the S334ter line-3 rat has a faster progression of degeneration than line-5. The horizontal and bipolar terminals are already affected at P11-P13 in both models. Apoptosis is related to the mutated rhodopsin transgene; the first photoreceptor cells affected are those close to the OPL.

© 2010 Elsevier Ltd. All rights reserved.

1. Introduction

Retinitis Pigmentosa (RP) is a group of inherited mutations causing photoreceptor degeneration, loss of night vision and blindness (review Berger et al., 2010; Lin and LaVail, 2010). In the developed world, about 1:3500 people are affected.

A subgroup of RP involves mutations of photoreceptor proteins. More than 25% of the autosomal dominant RP cases are caused by rhodopsin mutations (Rosenfeld et al., 1992; Shastry, 1994; Sohocki et al., 2001; Wang et al., 2001, 2005). As a model for RP, several rat lines have been created expressing mutant human rhodopsins (Steinberg et al., 1996). The *S334ter* mutation causes the formation of a truncated rhodopsin that is not trafficked to the outer segments (Green et al., 2000; Lee and Flannery, 2007). Heterozygous rats of the fast degenerating line *S334ter* line-3 never develop rod photoreceptor outer segments and show photoreceptor degeneration starting from P11 (Liu et al., 1999; Li et al., 2010), whereas retinal degeneration occurs after full retinal development in the *S334ter* line-5 rat (Thomas et al., 2004; Pennesi et al., 2008). However, the *S334ter* line-5 rat never develops a normal ERG (LaVail, personal communication; Thomas et al., unpublished results).

In retinal degeneration, the loss of photoreceptors affects the morphology and synaptic connectivity at the outer and inner plexiform layers (OPL, IPL) (Cuenca et al., 2004, 2005) (review Jones

and Marc, 2005; Marc et al., 2007). In advanced disease, these changes can be extensive, with marked disorganization and rewiring of the remaining inner retinal neurons (Jones et al., 2003; Marc et al., 2003; Strettoi et al., 2003). This process is thought to be due to denervation of the inner retinal neurons and subsequent attempts by these neurons to find new synaptic inputs. It involves cell death, rewiring (formation of new circuits to replace lost innervation) and cell migration.

Although the *S334ter* line-3 rat has been used in different experimental paradigms (An et al., 2002; Sagdullaev et al., 2003; Pennesi et al., 2008; Seiler et al., 2008a,b, 2010), only few studies about the *S334ter* line-5 have been published (Thomas et al., 2004; Pennesi et al., 2008).

The aim of this study was to compare the changes in the inner retina in these two different retinal degeneration models and to investigate the mechanism of retinal degeneration in order to establish which model would be more suitable for different experimental therapy studies.

2. Materials and methods

2.1. Experimental animals

All animals were maintained in accordance with the NIH statement for the use of animals in research, and the research was approved by the Animal Care and Use Committee of the University of Louisville, University of Southern California, and University of Alicante. Animals studied included three pigmented *S334ter* line-3, and three albino line-5 for each time point at P11–13, P30, P60, P90; two Long-Evans (LE) rats as controls for *S334ter* line-3 and two Sprague–Dawley rats as controls for *S334ter* line-5 (both at P60). The transgenic *S334ter* rats were produced by Xenogen Biosciences (formerly Chrysalis DNX Transgenic Sciences, Princeton, NJ), and developed and supplied with the support of the National Eye Institute by Dr. Matthew LaVail, University of California San Francisco (http://www.ucsfeye.net/mlavailRDratmodels.shtml). Pigmented heterozygous *S334ter* line-3 rats were a cross between homozygous albino line-3 rats and Copenhagen rats (Harlan, Indianapolis, IN). The rats were bred on a pigmented background for other experimental reasons (electrophysiological and optokinetic testing). Since there are no homozygous line-5 rats available, heterozygous line-5 rats were bred either among themselves or with albino Sprague-Dawley rats. The offspring was genotyped by PCR for the *S334ter* rhodopsin transgene.

2.2. Tissue processing

For immunohistochemistry, at least three animals were studied at each time point. Animals were killed with a lethal dose of pentobarbital, and the eyes were enucleated and immersion-fixed with 4% paraformaldehyde for two hours at 4 °C, and then washed with 0.1 M Na-phosphate buffer, pH 7.2. The eyes were cut in dorso-ventral orientation, and the lens removed. The eye cups were then placed in a small cryovial in 30% sucrose in 0.1 M Na-phosphate buffer, left there overnight, frozen in isopentane on dry ice and shipped to the University of Alicante. Sixteen μm thick cryostat sections (Leica CM 1900, Leica Microsystems) were mounted on Plus glass slides.

2.3. Immunohistochemistry

For blocking non-specific staining, sections were incubated in 10% normal donkey serum for 1 h (Jackson, West Grove, PA, USA) with 0.5% Triton X-100 and then incubated overnight at room temperature with combinations of different primary antibodies diluted in PBS containing 0.5% Triton X-100. All primary antibodies used in this study had been previously shown to be useful in the rat retina (Table 1). Subsequently, the sections were washed in PBS and incubated in the secondary antibodies, Alexa Fluor 488-conjugated donkey anti-rabbit IgG (green) and Alexa 546-conjugated donkey anti mouse IgG (red, Molecular Probes, Eugene, OR, USA) at a 1:100 dilution for 1 h. The sections were finally washed in PBS, mounted in fluoromount Vectashield (Vector Laboratories) and coverslipped for viewing by laser-confocal microscopy (Leica TCS SP2 Leica Microsystems). Immunohistochemical controls were performed by omission of either the primary or secondary antibodies. Unless otherwise indicated, images were obtained from central retinal sections. Final images were created from the projections of four to six single frames. TIFF images were enhanced using Adobe Photoshop CS3.

2.4. PNA label

For labeling of cone photoreceptors, sections were incubated in fluorescein isothiocyanate (FITC)-conjugated PNA (FITC-PNA, 1:400, Vector Labs, Burlingame, CA) for 1 h, after rhodopsin primary antibody for double labeling and 1 h alone for single labeling.

2.5. TUNEL label

Apoptosis was analyzed by the terminal deoxynucleotidyl transferase-mediated fluorescein-dUTP nick-end labeling (TUNEL) technique using the In Situ Cell Death Detection Kit from Roche Applied Science (Penzberg, Germany).

Table 1
Primary antibodies.

Molecular marker	Specific for	Antibody (reference)	Source	Working dilution
Calbindin D-28 K	Horizontal cells	Rabbit polyclonal (Cuenca et al., 2004)	Swant (Bellinzona, Switzerland)	1:500
Protein kinase C, α isoform (PKCα)	Rod bipolar cells	Rabbit polyclonal (Pinilla et al., 2007)	Santa Cruz Biotechnology (Santa Cruz, CA, USA)	1:100
Protein kinase C, α isoform (PKCα)	Rod bipolar cells	Mouse, clone MC5 (Johnson et al., 2003)	Santa Cruz Biotechnology	1:100
Recoverin	Photoreceptors; cone bipolar cells	Mouse monoclonal (McGinnis et al., 1997)	J.F. McGinnis, University of Oklahoma (Oklahoma City, OK,USA)	1:2000
Transducin, γ subunit	Cones and subpopulation of cone bipolars	Rabbit polyclonal (Peng et al., 2003; Zhang et al., 2003)	Cytosignal (Irvine, CA, USA)	1:200
Bassoon	OPL: ribbon synapses; IPL: conventional amacrine synapses	Mouse monoclonal (Brandstatter et al., 1999)	Stressgen (Ann Arbor, MI, USA)	1:5000
Parvalbumin	A-II amacrine cells	Rabbit polyclonal (Wässle et al., 1993; Cuenca et al., 2005)	Swant (Bellinzona, Switzerland)	1:300

3. Results

3.1. Photoreceptors and subtypes of cone bipolar cells (Recoverin, cone transducin, rhodopsin and PNA) (Figs. 1–5)

The outer nuclear layer (ONL) including cones and rods in normal control LE and SD rats, stained strongly for recoverin (Fig. 1A,B,D,E). In addition, two types of cone bipolar cells are labeled with antibodies against recoverin. Type 2 OFF-cone bipolar cells have large somata and strong immunoreactivity in their cell bodies located in the center of the inner nuclear layer (INL) (Fig. 1A,B,D,E arrows) with a dense continuous plexus of axons terminating in the sublamina a of the inner plexiform layer (IPL) (small arrows); and Type 8 ON-cone bipolar cells have small somata (Fig. 1A,B,D,E *arrowheads*) and their diffuse plexus of axons ends in sublamina b of the IPL close to the ganglion cell layer (GCL) (Fig. 1A,B,D,E small *arrowheads*) (Euler and Wässle, 1995; Cuenca et al., 2004).

Transducin γ-subunit is a cone marker (Peng et al., 2003). The antibody against cone γ-transducin labeled cone cell bodies, axon terminals and outer segments (Fig. 1B,C,E,F). Cone cell bodies are located in the outer most rows of the ONL. In addition, a more faintly stained subpopulation of cone bipolar cells and terminals in the IPL were labeled with γ-transducin antibodies (Fig. 1B,E). One of these subpopulations corresponds to the Type 8 ON bipolar cells because they are also immunoreactive for recoverin (Fig. 1B,E arrowheads).

In normal SD retina, antibodies against rhodopsin only stain rod outer segments (Fig. 1G,H). Peanut agglutinin (PNA) label showed cones outer segments (Fig. 1H,I). Similar results were seen in LE retinas (data not shown).

At P11, *S334ter* line-3 rats still contained a full-thickness ONL (Fig. 2A). All rod cell bodies stained for rhodopsin (Fig. 4A). Rods contained inner segments, but no developed outer segments (Fig. 2C). Cone cell bodies were present in the center of the ONL, but with only few and short outer segments (Fig. 2B,C) as confirmed by PNA stain (Fig. 5A). Some ectopic rod nuclei could be identified on top of the inner segments (Fig. 2C arrows).

The ONL in line-5 rats looked normal at P13 (Fig. 3A). Rod inner and outer segments could be identified, but cone cell bodies were located in the middle of the ONL; their outer segments were better developed than in line-3 (Fig. 3B,C arrowheads). Similar to line-3, line-5 rod cells bodies all stained for rhodopsin (Fig. 4B). Cone outer segments stained with PNA appeared longer than in line-3 (Fig. 5B).
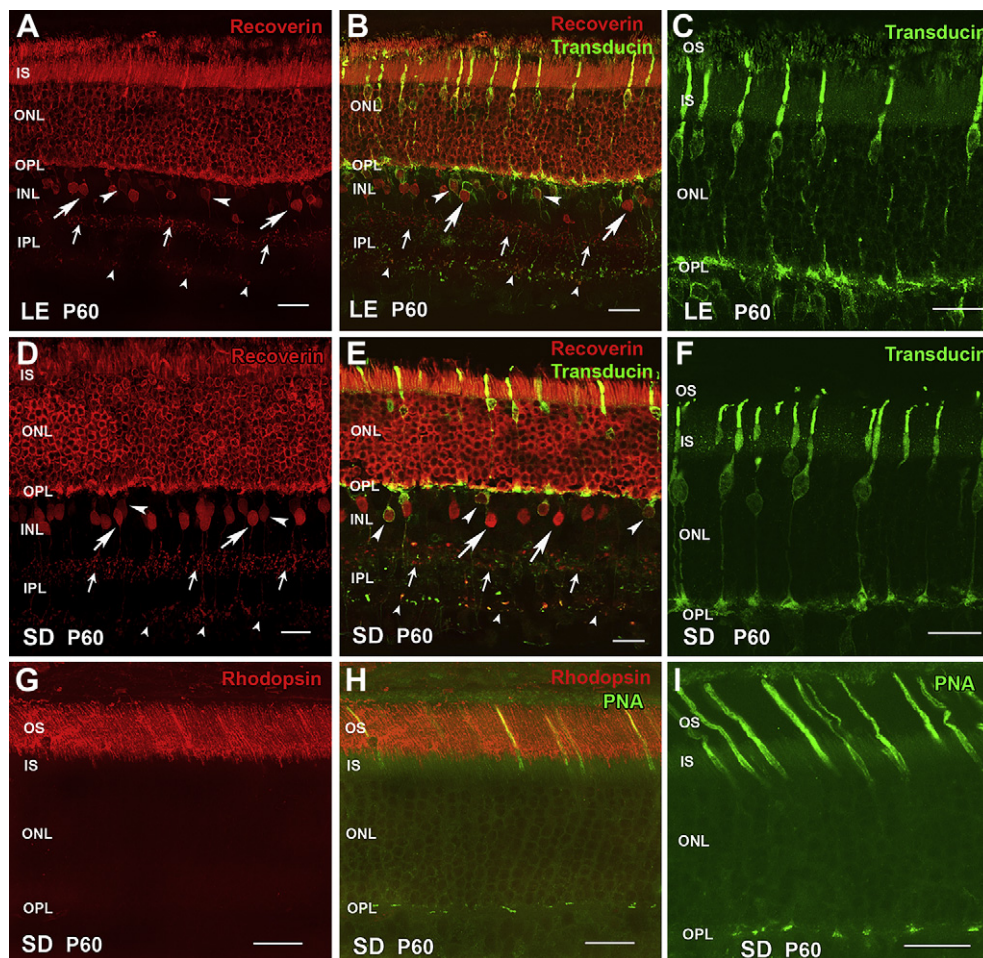

Fig. 1. Normal retina controls − Photoreceptors (recoverin, cone transducin, rhodopsin, PNA) and cone bipolar cells (recoverin). (A–C) Long-Evans (LE) rat (control for *S334ter-3*). (D–I) Sprague–Dawley (SD) rat (control for *S334ter-5*). (A,B,D,E): Recoverin (labels photoreceptors and cone bipolar cells). Large arrows point to type 2 OFF cone bipolar cells with large somata; small arrows indicate their axon terminals in sublamina a of the IPL. Arrowheads point to type 8 ON cone bipolar cells with smaller somata; small arrowheads indicate their terminals in sublamina b of the IPL. (B,E): Recoverin (red)/cone transducin (green). (C,F): cone transducin (green; higher magnification). Cone cell bodies are localized close to the outer limiting membrane. Outer segments and cone pedicles are clearly labeled. G,H) rhodopsin (red) stains only rod outer segments in a normal SD rat. H,I) Peanut agglutinin (PNA, green) labels the extracellular matrix around cone outer segments. Magnification bars = 20 μm.
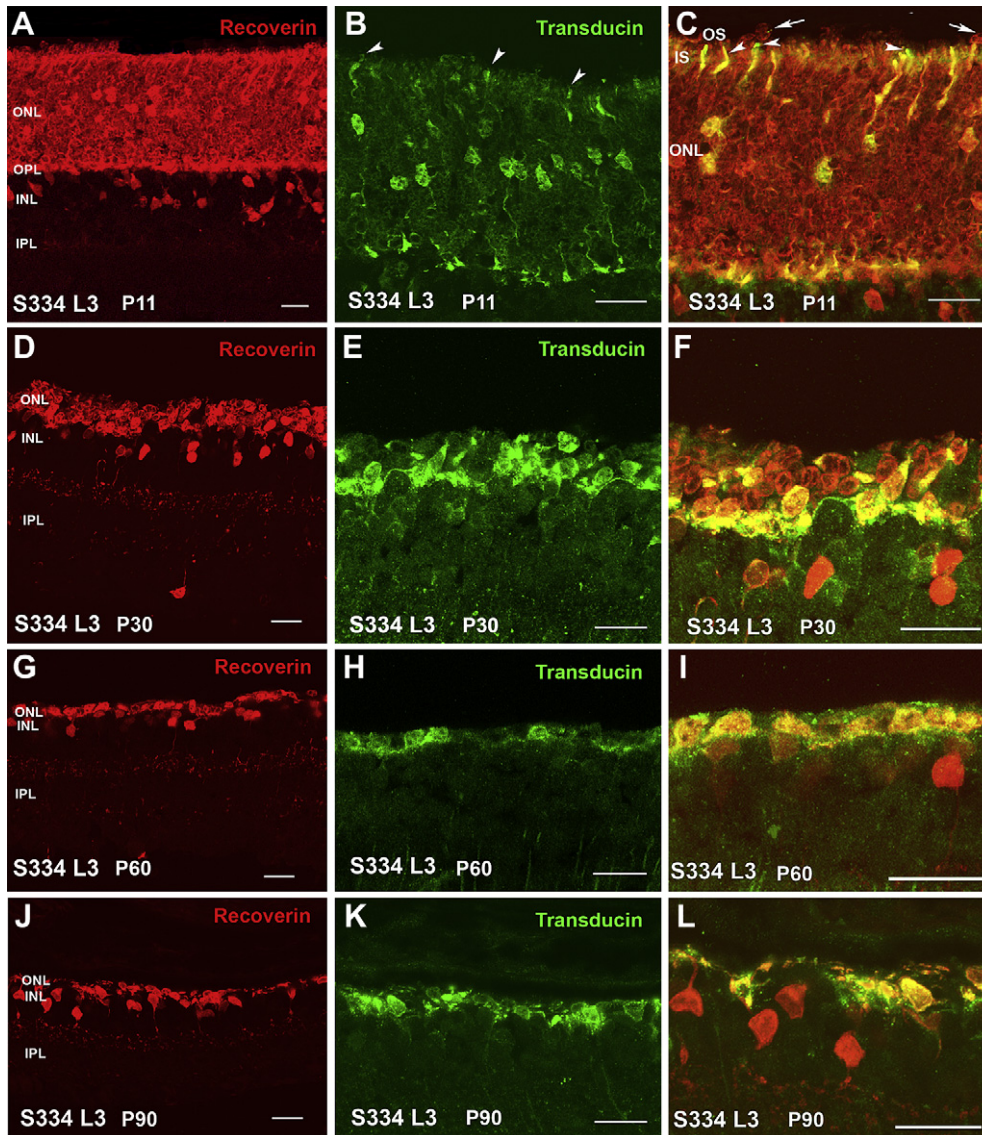
Fig. 2. Photoreceptor degeneration in *S334ter* line 3. Left column (A,D,G,J): recoverin (red); middle column (B,E,H,K): cone transducin (green); right column (C,F,I,L): double staining recoverin/cone transducin. (A–C): At P11, the photoreceptor layer shows full thickness, but without rod outer segments (A,C) and only few short cone outer segments (B,C). (C) Double label recoverin (red)/transducin (green). Arrows point to ectopic rod cells outside ONL. Arrowheads indicate cone outer segments. (D–F): At P30 there are approximately 2 layers of nuclei in the ONL, and no outer segments. (E): Cone cell bodies look disorganized without outer segments and are randomly distributed, not lined up close to outer limiting membrane. (F): Remaining rods appear red, remaining cones yellow. (G–I): At P60, the ONL is reduced to one, non-continuous layer of nuclei with only cones which appear yellow in recoverin/transducin double stain. (J–K): Further degeneration at P90: Remaining cones sprout processes at the outermost edge of the retina. Magnification bars = 20 μm.

Line-3 rats exhibited a faster rate of degeneration with an early loss of photoreceptors, with two layers of nuclei remaining in the ONL at P30 (Fig. 2D,F). At this age, in the remaining photoreceptors, no outer or inner segments could be identified. Double labeling with recoverin and transducin showed one to two rows of rods (red cells) (Fig. 2F) which was confirmed by rhodopsin staining (Fig. 4C). Cones (yellow cells in Fig. 2F) appeared completely disorganized in the line-3 rat at P30, with short remnants of outer segments and abnormal morphology of axon terminals (Figs. 2E,F and 5C).

Line-5 rats had still 4–5 layers of nuclei in the ONL remaining at P30, but with distorted outer segments (Fig. 3D,F; Fig. 4D). Cones at this age still had a bipolar appearance with small size shortened outer segments and axon terminals (Fig. 3E,F), and short outer segments (Fig. 5D). Cone bipolar cells still made synaptic contacts with cone pedicles (Fig. 3F turquoise arrowheads).

At P60 and P90 in line-3, only one row of photoreceptors could be identified at the ONL (Fig. 2G,J). Double immunolabeling with recoverin and γ-transducin showed that only cone cells remained at this age (yellow, double staining with the two markers) and no rods were present (Fig. 2I–L). However, rhodopsin staining identified very few rods without any cell processes (Fig. 4E) only in the central retina. Cones appeared to be oriented horizontally and only cell bodies could be identified (Fig. 2H,I,K,L) which had lost their PNA stain (Fig. 5E).

Line-5 had one row of photoreceptors at P60 and P90 (Fig. 3G,J). Most of the remaining photoreceptors were cones (Fig. 3H,K). Double labeling with recoverin and γ-transducin (Fig. 3I,L arrows) and rhodopsin immunostain (Fig. 4F) showed a few rods remaining in line-5 at P60-90 exhibiting rhodopsin immunoreactivity concentrated along the complete cell body (Fig. 4F). Cones at P60 and P90 had a distorted morphology but outer segments could still
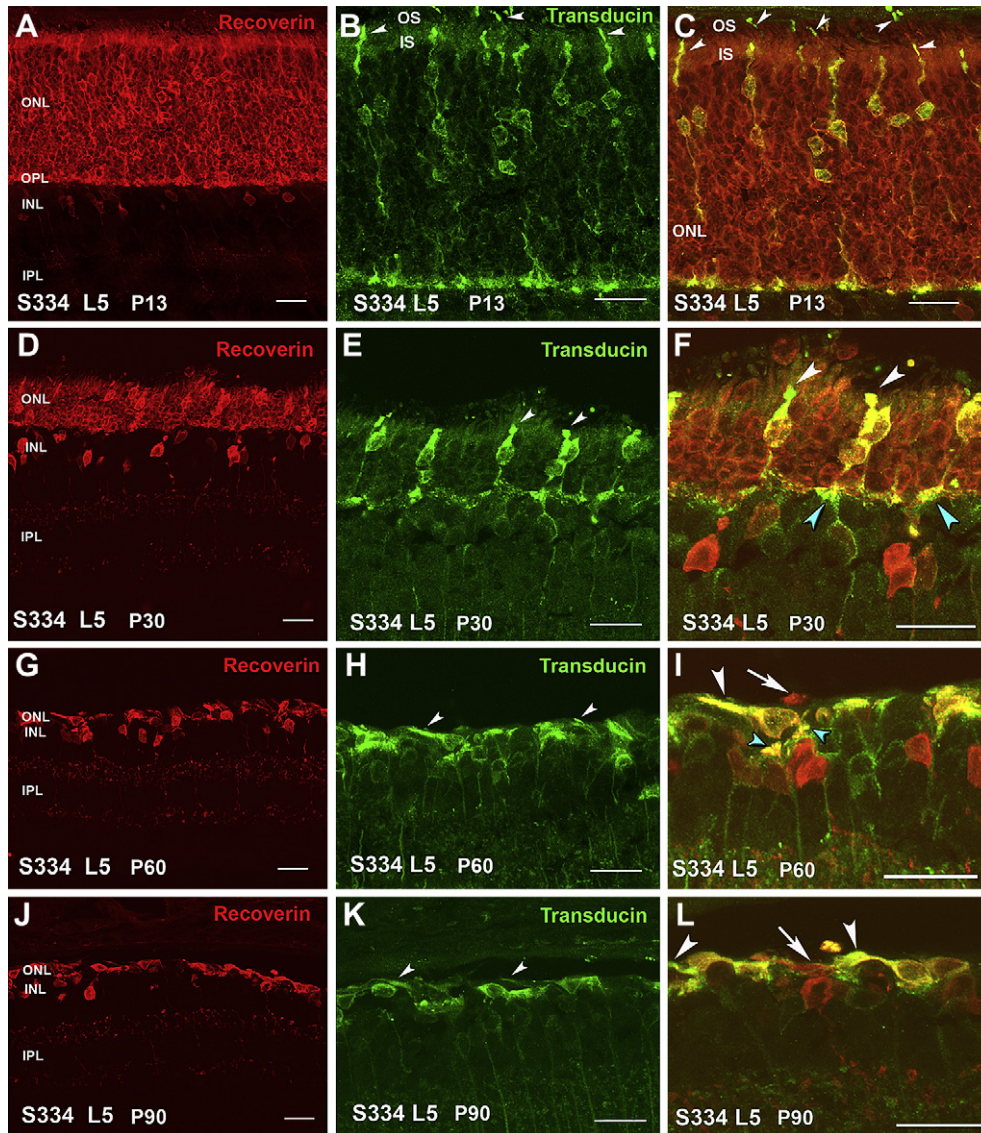
Fig. 3. Photoreceptor degeneration in *S334ter* line 5. Left column (A,D,G,J): recoverin (red); middle column (B,E,H,K): cone transducin (green); right column (C,F,I,L): double staining recoverin/cone transducin. White arrowheads indicate cone outer segments; turquoise arrowheads indicate synapses between cone pedicles and cone bipolar cells; arrows in (I) and (L) indicate remaining rods. (A–C): At P13 the photoreceptor layer is fully developed, with short rod outer segments (A) and prominent cone outer segments (B,C, arrowheads). (B,C): Cone outer segments and pedicles are more strongly stained than in line-3. − (D–F): At P30 there are approximately 4–5 layers of nuclei in ONL, short outer segments. (F): Cones (yellow) are still regularly arranged close to the outer limiting membrane, with stubby outer segments. Remaining rods appear red. − (G–I): At P60, the ONL is reduced to one, non-continuous layer of cone nuclei. Cone cell bodies are oriented parallel to the outer limiting membrane. (J–L): Further degeneration at P90. Magnification bars = 20 μm.

be recognized (Fig. 3H,I,K,L white arrowheads; Fig. 5F) and cone bipolar cells made synaptic contacts with remaining cone pedicles (Fig. 3I turquoise arrowheads).

3.2. Horizontal, bipolar, and A-II amacrine cell changes in relation to photoreceptor and synaptic loss (Figs. 6–9; Supplemental Figs. S1–S3) (calbindin, PKC, recoverin, rhodopsin, parvalbumin, bassoon)

Horizontal cells can be identified using antibodies against calbindin. In control rat retinae (Fig. 6A,B), the dendrites of the single horizontal cell type, the B-type cell, contact cone terminals, and the axon terminal contacts rod terminals in the outer plexiform layer (OPL). The terminal tips making synaptic contact with spherules of rods and pedicles of cones are easy to identify in LE (Fig. 6A arrowheads) and SD rats (Fig. 6B arrowheads).

At P11–13, in both *S334ter* transgenic lines, the regular and dense plexus of horizontal cells processes and tip terminals in the OPL was different from control retinas and there was a clear reduction of dendrites and axon terminal tips (Fig. 6C,D). However, horizontal cells dendrites appear to be less complex in line-3 than in line-5. Horizontal cell processes were gradually diminished between P11–13 and P30, both in line-3 (Fig. 6C,E) and in line-5 (Fig. 6D,F). In line-5, calbindin-immunoreactive terminal tips could be identified (Fig. 6F arrowheads); however, in line-3, clear terminal tips were difficult to recognize at P30 (Fig. 6E).

At P60, the horizontal cell plexus showed gaps in the OPL in both lines (Fig. 6G,H). Almost no terminal tips could be seen in line-3 (Fig. 6G) and a few of them could be observed in line-5 (Fig. 6H arrowheads). At P90, no terminal tips were found. The horizontal cell plexus was almost gone in line-3 (Fig. 6I) and a few processes remained in line-5 (Fig. 6J).
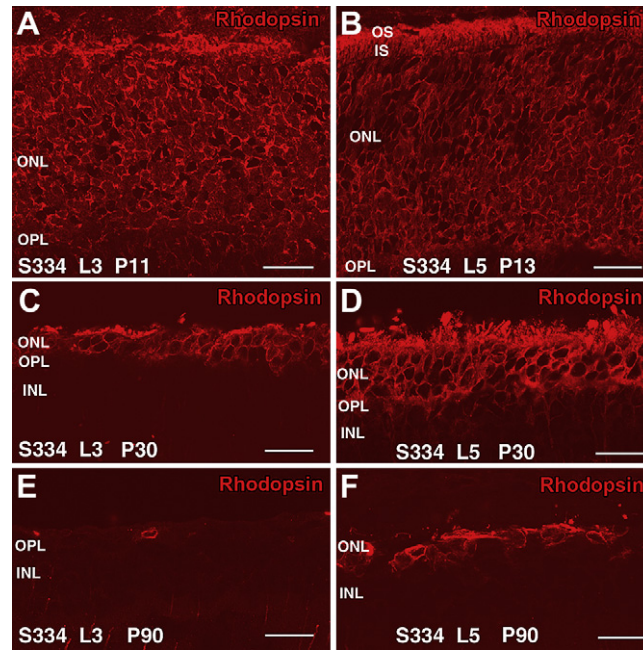
Fig. 4. Rhodopsin stain in line-3 (A,C,E) and line-5 (B,D,F) retina. A) Line-3 at P11: rod photoreceptor cell bodies stain abnormally for rhodopsin. No developed rod outer segments. B) Line-5 at P13: abnormal rhodopsin stain of rod cell bodies, short rod outer segments. C) Line-3 at P30: few rods left. D) Line-5 at P30: four rows of rods left with distorted outer segments. E) Line-3 at P90: No rods left, except for one cell body without any cell processes. No rod outer segments. F) Line-5 at P90: One row of rods left. No recognizable rod outer segments. Magnification bars = 20 μm.

In normal SD retina at P60, a single type of rod bipolar cells is PKC (protein kinase C alpha) immunoreactive. The ON-rod bipolar cell bodies were mostly aligned in the outermost part of the INL. Each rod bipolar cell had a single primary dendrite and a tuft of dendritic terminals contacting rod cells. Their single axon ran perpendicularly through the IPL ending in stratum S5 of the IPL as large axon terminal end-bulbs together with some lateral terminal varicosities, close to the ganglion cell layer (Supplemental Fig. S1A).

During the course of photoreceptor degeneration in line-5, ON-rod bipolar cell terminals in the IPL showed decreased staining intensity at P32 and P60 (Supplemental Fig. S1 B,C). In addition, their dendritic terminals appeared to be reduced in length and in density (Supplemental Fig. S1 B,C). The entire length of their cell body was reduced by P60.

Because of the close relationship between rod bipolar cells and A-II amacrine cells, it was important to see whether A-II amacrine
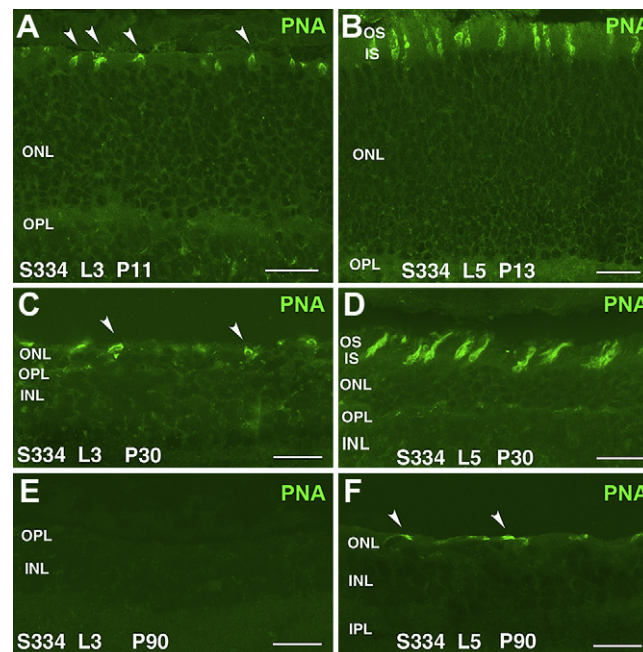

Fig. 5. PNA stain in line-3 (A,C,E) and line-5 (B,D,F) retina. A) Line-3 at P11: Very short cone outer segments (arrowheads). B) Line-5 at P13: Cone outer segments appear longer and more numerous than in line-3. C) Line-3 at P30: Reduced number of short cone outer segments (arrowheads). D) Line-5 at P30: Short cone outer segments; density similar to P13. E) Line-3 at P90: no PNA stain. F) Line-5 at P90: PNA staining of distorted short cone outer segments (arrowheads). Magnification bars = 20 μm.
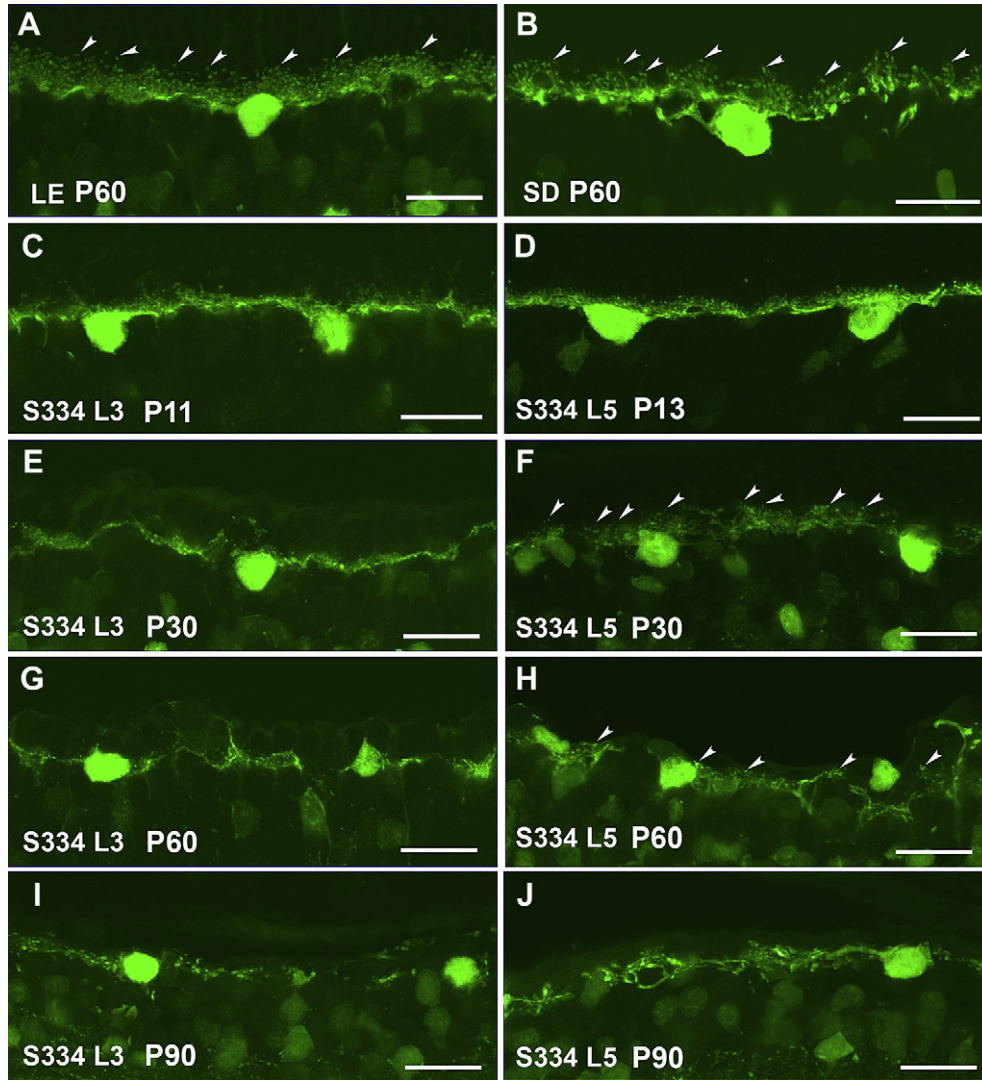
Fig. 6. Horizontal cells (calbindin). Normal Long-Evans and Sprague-Dawley rat (A,B) compared with *S334ter-3* rats (C,E,G,I) and *S334ter-5* rats (D,F,H,J):. Arrowheads in A,B,F,H indicate terminal tips, making synaptic contacts with spherules of rods and pedicles of cones. (C,D) Relatively normal morphology of horizontal cells at P11–13. At later ages (P30: E,F; P60: G,H; and P90: I,J), the morphology of horizontal cell dendrites deteriorates in both transgenic strains. Magnification bars = 20 μm.

cells also changed with time. In normal SD retina, A-II amacrine cells exhibit a characteristic morphology conserved in all mammals that can be identified upon immunostaining for parvalbumin, a calcium-binding protein that constitutes an excellent phenotypic marker for this neuronal type in rat retina. A-II amacrine cells bear a mitral-shaped cell body, located in the innermost INL stratum, and a primary, stout dendrite from which lobular appendages full of mitochondria emerge restricted to sublamina a of the IPL (Fig. 7A,B
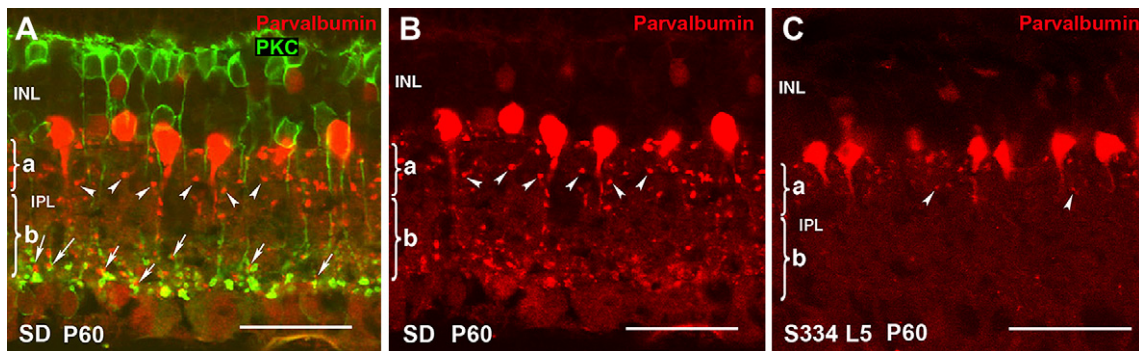

Fig. 7. Rod bipolar cells and A-II amacrine cells of normal SD rat (A,B) compared with *S334ter-5* rat (C). (A) PKC/parvalbumin: Normal SD rat at P60. Arrows point to A-II amacrine – rod bipolar synapses in IPL, close to ganglion cells (sublamina a). (B) Parvalbumin, normal SD rat at P60: arrowheads point to synaptic terminals in IPL sublamina a. (C) Parvalbumin, *S334ter-5* at P60: A-II amacrine cells appear shrunken; no synapses labeled in IPL sublamina b, reduced synapses in sublamina a. Magnification bars = 40 μm.
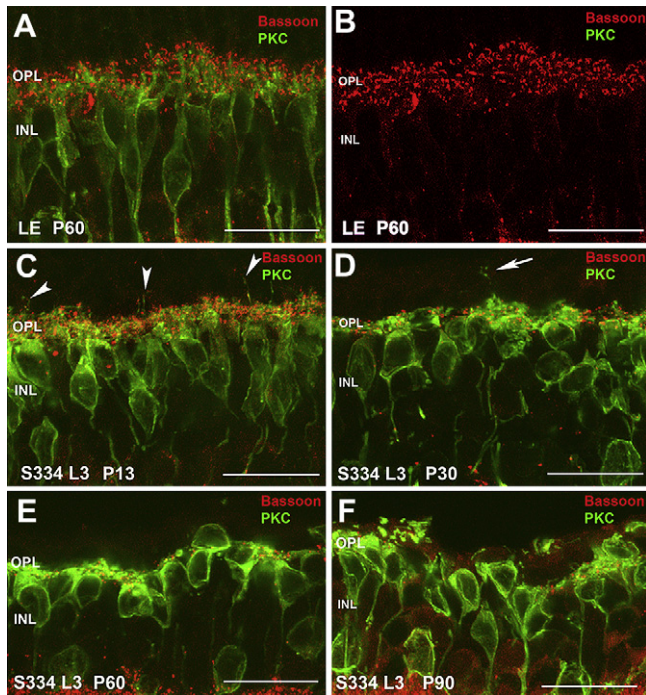
Fig. 8. Normal Long-Evans rat (LE; A, B) compared with S334ter-3 rat (C-F): Rod bipolar cells (PKC, green) and ribbon synapses (bassoon, red). (A) Normal LE rat. At high magnification, the interaction of rod bipolar cell dendrites (green) with photoreceptor ribbon synapses (red) can be seen. (B) shows the same image of just the red bassoon channel. (C) Higher magnification of Supplemental Fig. S2 C: At P11, there are still numerous photoreceptor ribbon synapses interacting with rod bipolar dendrites. Arrowheads point to bipolar cell dendrites sprouting into the ONL. (D) Higher magnification of Supplemental Fig. S2D): at P30, most photoreceptor synaptic ribbons have been lost. There is abnormal sprouting of bipolar cell dendrites (arrow). (E) Few photoreceptor ribbon synapses left at P60. F) Almost complete loss of photoreceptor ribbon synapses at P90. Aberrant retraction of bipolar cell dendrites that are clumped together. Magnification bars = 20 μm.
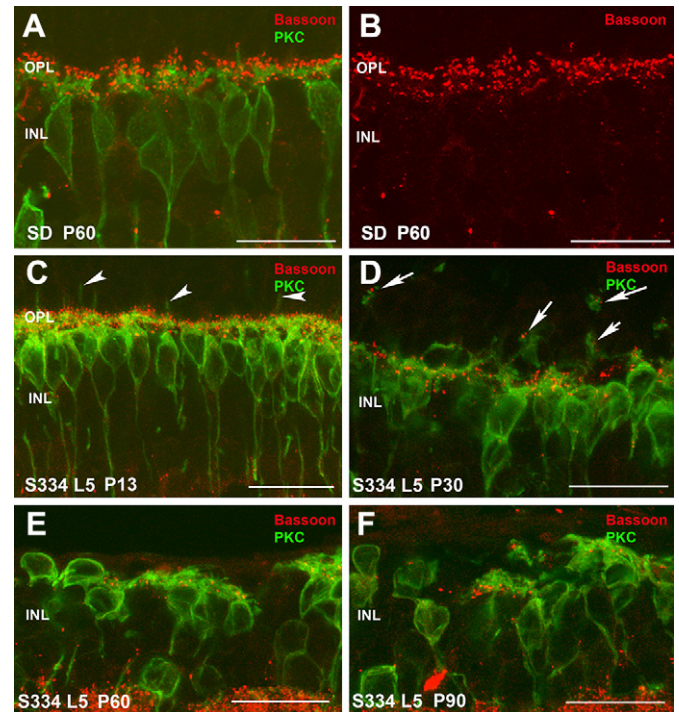
Fig. 9. Normal Sprague—Dawley rat (SD; A,B) compared with *S334ter-5* rat (C-F): Rod bipolar cells (PKC, green) and synapses (bassoon, red). (A) At high magnification, the interaction of rod bipolar cell dendrites (green) with photoreceptor ribbon synapses (red) can be seen. (B) shows the same image of just the red bassoon channel. (C) Higher magnification of Supplemental Fig. S 3C: at P13, there are still numerous photoreceptor synaptic ribbons interacting with rod bipolar dendrites. Arrowheads point to bipolar cell dendrites sprouting into the ONL. (D) Higher magnification of Supplemental Fig. S3 D: at P30, many photoreceptor ribbon synapses have been lost. There is abnormal sprouting of bipolar cell dendrites (arrows). - PKC/bassoon stain at P60 (E) and P90 (F): Further reduction of photoreceptor ribbon synapses, abnormal morphology of rod bipolar cells. Magnification bars = 20 μm.

arrowheads) (Voigt and Wässle, 1987; Kolb et al., 2002). Also, distal dendrites ramify down into sublamina b in the IPL where they receive excitatory inputs from rod bipolar cells (Fig. 7A arrows) and transfer the rod signal to the cone pathway by means of conventional, chemical synapses with OFF-cone bipolars and gap junction-mediated electrical synapses with ON-type cone bipolars. At P60 in line-5, A-II amacrine cells lost parvalbumin stain of their synaptic terminals completely in sublamina b and a few lobular appendages could be observed in sublamina a (Fig. 7C arrowheads). Line-3 rats showed similar, but faster changes (data not shown).

In order to identify the synaptic contacts between photoreceptors and rod ON-bipolar cells in the OPL during the degeneration of both lines, antibodies against bassoon and PKC were used. Bassoon is a presynaptic protein located at the synaptic ribbon in cone and rod terminals in the OPL. In the IPL, bassoon is concentrated at conventional GABAergic amacrine synapses but is absent from the bipolar cell ribbon synapses (Brandstatter et al., 1999). We used antibodies against PKC to identify the dendritic terminals of rod bipolar cells that represent one of the postsynaptic elements to rod photoreceptors.

Double labeling with bassoon and PKC showed the relationship between photoreceptors and rod bipolar cells. In LE rats (Fig. 8A,B; Supplemental Fig. S2 A,B) and SD rats (Fig. 9A,B; Supplemental Fig. S3A,B), dendritic terminals of rod bipolar cells (green) could be seen paired with red bassoon staining (Figs. 8A, 9A; Supplemental Figs. S2 A, S3 A). Figs. 8B and 9B show the typical horseshoe morphology corresponding to synaptic ribbon sites of rod spherules on rod ON- bipolar cells.

In contrast, in both lines 3 and 5 rats even by 11—13 days of age, changes were already evident (Figs. 8C, 9C; Supplemental Figs. S2C, S3C). The dendritic terminals of rod bipolar cells appeared to be reduced in length and in density. Some sprouting of their dendrites into the ONL had already started (Figs. 8C and 9C arrowheads). Bassoon immunoreactive spots on top of rod bipolar dendrites were also reduced and lost the typical horseshoe morphology. Rod bipolar cell bodies in line 3 had lost their typical alignment in the INL and their axons did not run perpendicular in the IPL compared with that seen in control and line 5 rats at this age (compare Fig. 8C with Fig. 9C; and Supplemental Fig. S2C with S3C).

At P30 in both lines (Figs. 8D, 9D; Supplemental Figs. S2 D, S3 D), rod bipolar cell shape and location was irregular compared with that seen in control retinas. The normal plexus of bipolar cell dendrites in the OPL was dramatically altered, and almost no secondary dendrites and terminal tips could be recognized. Bassoon immunoreactive spots were mostly lost and the few remaining were seen as dots in the atypical portion of the bipolar cell bodies. Some of the bassoon immunoreactivity spots were also associated with the sprouted dendritic terminals in the ONL (Figs. 8D and 9D, arrows) suggesting ectopic synapses.

With the progression of the degeneration at P60 (Fig. 8E; Supplemental Fig. S2 E for line-3 and Fig. 9E, Supplemental Fig. S3 E for line-5) and P90 (Fig. 8F, Supplemental Fig. 2 F for line-3 and Fig. 9F, Supplemental Fig. S3 F for line-5), rod bipolar cell bodies were highly irregular, some were even located upside down. Clear gaps between cell bodies suggested a loss of rod bipolar cells with time. Their dendritic branches were much diminished, and many

cells appeared without processes on their outer surface. The few immunoreactive bassoon spots found in the OPL at P60-P90 may correspond to the remaining degenerating cone pedicles.

During the time course from P11–13 to P90, the axonal arborizations of rod bipolar cells in the IPL were simpler and the terminal varicosities were smaller than in the control rats. The axons and the terminal varicosities had reduced size and immunoreactivity (Supplemental Fig. S2 C–F for line 3 and Supplemental Fig. S3 C–F for line 5).

3.3. Apoptosis (Fig. 10)

S334ter line-3 rats showed a significant number of photoreceptors affected at P11, occupying the innermost part of the ONL close to the OPL (Fig. 10A). Line-5 showed a lower number of apoptotic cells within the same location at P13 (Fig. 10B). At P30, most of remaining photoreceptor in line-3 rats were apoptotic (Fig. 10C), whereas the percentage of apoptotic nuclei in the ONL remained smaller in line-5 rats (which had still 4 rows of nuclei remaining) (Fig. 10D). In addition, in both lines, apoptotic nuclei were found in the ganglion cell layer. At later stages (data not shown), horizontal cells, cones, and more ganglion cells became apoptotic.

4. Discussion

This paper presents a detailed exploration of degenerative processes in the *S334ter* line-3 and, for the first time, in *S334ter* line-5 transgenic rat models. The results complement similar studies in *S334ter* line-3 rats (Hombrebueno et al., 2010; Li et al., 2010; Ray et al., 2010), *P23H* line-1 transgenic rats (Cuenca et al., 2004; Kolomiets et al., 2010), *RCS* rats (Cuenca et al., 2005), *rd* mice (Strettoi et al., 2003; Barhoum et al., 2008; Lin et al., 2009) and other retinal degeneration models (Jones et al., 2003; Sullivan et al.,

2003; Marc et al., 2008; Nagar et al., 2009) (review Jones and Marc, 2005; Marc et al., 2007).

4.1. S334ter mutation

Three transgenic rat lines with the *P23H* rhodopsin mutation and five lines with the *S334ter* rhodopsin mutation (derived from the albino Sprague–Dawley strain) were created in 1996 (Steinberg et al., 1996; Pennesi et al., 2008). *P23H* rats carry a single amino acid mutation at codon 23 of the opsin gene. *S334ter* transgenic rats express an opsin gene with a termination codon at residue 334, resulting in a C-terminal truncated opsin protein which cannot be phosphorylated. Two lines with relatively fast photoreceptor degeneration, lines 3 and 5, were selected for the current study. In the line 3 rat, the ONL is reduced to 2 layers at the age of 20 days whereas this stage is reached at the age of 60 days in the line-5 rat (Pennesi et al., 2008). With some opsin mutations, photoreceptor degeneration is faster in albino animals (Naash et al., 1996). Although it would have been ideal to compare lines with the same genetic background, the line-3 rats in our study were pigmented, in contrast to the original albino founders of this strain (Steinberg et al., 1996) because they were bred for transplantation studies and different functional tests which can only be performed in pigmented rats (e.g. optokinetic testing). Pigmented line-3 rats have been investigated in other studies (Hombrebueno et al., 2010; Ray et al., 2010).

4.2. Time course of photoreceptor degeneration

Although both transgenic rat models used in this study carry the same mutant human rhodopsin, *S334ter*, the time course of degeneration is different. Line-3 rod photoreceptors never develop outer segments whereas line 5 photoreceptors do. In both lines, rhodopsin immunoreactivity was found in rod cell bodies around P11–13 showing an early stage of degeneration, similar to what has been seen in other retinal degeneration models (Cuenca et al., 2004, 2005). However, at P13, there were numerous apoptotic cells in the ONL even in line-5 (before photoreceptor development was completed) corresponding to a previous study that showed a 50% reduction of the ONL in line-5 at P15 (Pennesi et al., 2008). Line-5 rod outer segments appeared normal at P13 but were already abnormal and distorted at P30 when more than 50% of the photoreceptors had died. At P60, there was not very much difference between the two models although some rod photoreceptors could still be found in line-5 and almost none in line-3. In comparison, photoreceptor degeneration in RCS rats takes 120 days (Cuenca et al., 2005) to reach a stage comparable to *S334ter* line-3 at P30 or S334 line-5 at P60. In homozygous *P23H* line-1 transgenic rats, this stage is reached after 150 days and later (Cuenca et al., 2004). In *S334ter* line-3 (albino) rats, Peanut agglutinin (PNA) staining of retinal wholemounts at P10 showed that outer segments of cones are present and cover the whole retina, but start to drop out at P20–30, and are reduced to few spots at P60-90 (Li et al., 2010). Our results showed that in *S334ter* line-3 pigmented rats at P11, cone cell bodies are displaced to the center of the ONL and that cone outer segments are present but shorter than in normal rats. We were not able to identify any PNA stain at P90 in line-3. Using S-opsin immunohistochemistry, it has been demonstrated that in pigmented line-3, cone photoreceptors completely change to an amacrine-like morphology and lack outer segments at P180 (Hombrebueno et al., 2010). In albino *S334ter* line-5 although cone cell bodies are also localized in the middle of the ONL, the outer segments of cones look normal and keep a rudimentary morphology at least until P90. These data indicate that line-3 rats do not develop normal cone outer segments, but line-5 rats reach the normal photoreceptor morphology by P13.
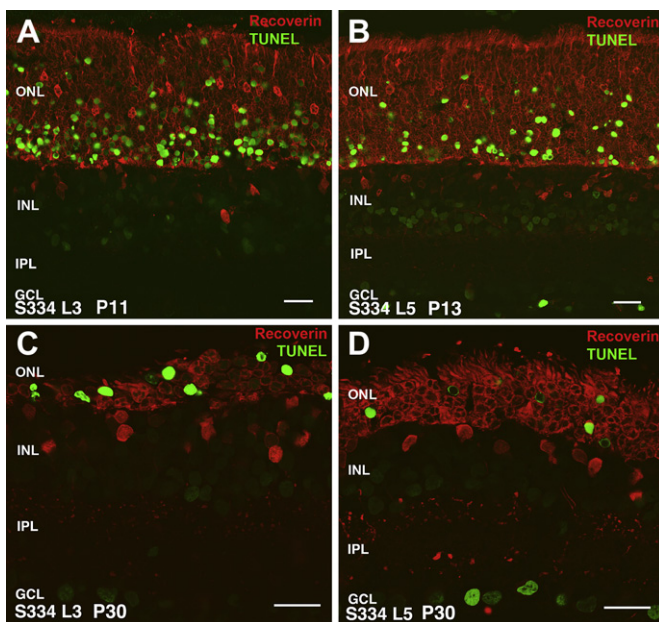

Fig. 10. Apoptosis (TUNEL stain, green) in combination with recoverin stain (red), comparison of line-3 (A,C) with line-5 (B,D). (A) *S334ter-3* rat at P11. Numerous TUNEL+ cells in ONL. (B) *S334ter-5* rat at P13: Strong TUNEL stain in ONL, but less cells than in line 3. (C) *S334ter-3* rat at P30: strong TUNEL stain in remnant of ONL. ONL reduced to 2-3 layers of nuclei. Faint stain of some cells in INL and GCL. (D) *S334ter-5* rat at P30: Thicker ONL (5 layers of nuclei) − strong TUNEL stain of cells in ONL. In addition, some cells in GCL are also strongly TUNEL stained. Fainter stain of cells in INL and GCL. Magnification bars = 20 μm.

4.3. Changes in outer plexiform layer and inner retina

A major purpose of the present study was to examine how synaptic contacts between photoreceptors and their postsynaptic elements were differentially affected by progressive loss of photoreceptors in line 3 and 5.

The loss of photoreceptor terminals in the OPL (indicated by bassoon staining) was reflected in the reduction of calbindin immunoreactive horizontal cell dendrites. The density of horizontal cells appeared to be reduced by P90 in both lines. A recent study quantified the density of horizontal cells in wholemounts of pigmented *S334ter* line-3 rat retinas at P60 and P90 and found a significant reduction in the central, not the peripheral retina (Ray et al., 2010). In the RCS rat, horizontal cells sprout processes into the INL at P90 (Cuenca et al., 2005); similar findings could be found in *rd*10 mice at P20, in which horizontal cells send similar processes into the INL surrounding the blood vessels (Barhoum et al., 2008). In these two *S334ter* rhodopsin-mutants of the current study, this was not observed to this extent.

Rod bipolar cells responded to photoreceptor death by loss of dendrites and aberrant sprouting into the ONL (as long as it was present). Sprouting is a common finding in retinal degenerative disease. After the loss of the photoreceptor cells, both bipolar and horizontal cell dendrites try to find synaptic inputs in the remaining cells. This change is a general finding in RP models but is very evident in the RCS rats, where the dendrites try to find a contact into the debris zone (Cuenca et al., 2004). These changes can be prevented with cell based photoreceptor rescue therapy and could be related to the preservation of the morphology of photoreceptors (Pinilla et al., 2007, 2009).

Retractions of dendrites of rod bipolar cells at P11-13 and the decrease of bassoon spots indicate that the synaptic contacts in the OPL were not well developed. The few bassoon immunoreactive dots on top of bipolar cell dendrites and the more irregular alignment of their cell bodies and axons in line-3 than in line-5 also indicate the slower degeneration of line-5. The changes at the OPL synaptic contacts are related to the rate of photoreceptor loss. However, in some models, such as short hyperoxia models in rodents, with a well developed ONL and a preserved number of cells, changes between photoreceptors and their postsynaptic neurons could be found at early stages with not evident changes in rods or cones (Dorfman et al., 2006). In addition, there were changes in rod bipolar cell terminals which showed changes in the IPL already at P11−13 when most photoreceptors were still present in both lines. At later stages, bipolar cell bodies migrated within the INL. It is known that rod bipolar cells make ectopic connections to cones after rod photoreceptor death (Peng et al., 2003; Cuenca et al., 2004; Strettoi et al., 2004; Marc et al., 2007).

4.4. Changes in A-II amacrine cells

Parvalbumin-immunoreactive A-II amacrine cells are major interneurons of the rod pathway and make synaptic connections between rod bipolar cells and cone bipolar cells (Voigt and Wässle, 1987; Wässle et al., 1993). At P60 in the *S334ter* line-5 rat, A-II amacrine cells were directly affected by the loss of synaptic input from rod bipolar cells with loss of parvalbumin immunoreactivity of most synaptic terminals in the IPL. Our results could not determine whether the processes regressed or changed their parvalbumin expression. Similar changes have been observed at P270 in the *P23H* line 1 transgenic rat (Cuenca et al., 2004) and at P30 in *rd*10 mice (Barhoum et al., 2008).

4.5. Cell death

Similar to what has been observed in other studies (Liu et al., 1999; Ray et al., 2010), our study showed that photoreceptor apoptosis appears in early stages in line-3 rats, with a great number of apoptotic cells at P11. Line-5 showed a slower death rate with 4 rows of cells surviving around P30. Fast retinal degenerative models, such as the *rd*10 mouse, show an early apoptotic peak, around P20 (Barhoum et al., 2008). In the ONL, apoptosis affected the rods first closest to the OPL. This is different to the RCS rat where apoptotic nuclei are seen throughout the ONL with no selective location (Martinez-Navarrete et al., 2006) (unpublished data). The location was the same in both pigmented line-3 rats and albino line-5 rats, so pigmentation had not a preventive effect of the cell death. Cones were affected only after all rods had died consistent with the type of mutation. In contrast to another study of the *S334ter* line 3 rat (Ray et al., 2010), our study found indications for apoptosis in inner retinal neurons and ganglion cells after degeneration of photoreceptors. In the *P23H* line-1 model of retinal degeneration, there is a progressive loss of retinal ganglion cells, but the remaining cells are still functional at the age of 12−16 months when no light responses can be recorded (Kolomiets et al., 2010). Several studies in different other retinal degeneration models (*rd* 10 and *rd* 1 mice) have also found that retinal ganglion cells survive long-term, maintain normal morphology and remain functional (Margolis et al., 2008; Mazzoni et al., 2008; Jensen and Rizzo, 2009).

5. Summary

In both investigated rat models of retinal degeneration, changes in rod bipolar and horizontal cells could be observed before complete rod photoreceptor death. Surviving cones persisted in the retina up to the oldest age studied (P90) and longer (Hombrebueno et al., 2010; Li et al., 2010). Both models show a similar pattern of degeneration and remodeling to other investigated rhodopsin mutants, (e.g. *P23H* line-1, *S334ter* line-4) but in a shorter time frame. The S334ter-3 model has been used in many experimental studies (An et al., 2002; Sagdullaev et al., 2003; Pennesi et al., 2008; Seiler et al., 2008a,b, 2010; Li et al., 2010; Ray et al., 2010). Because line-3 rats do not reach normal photoreceptor morphology, fewer horizontal processes and bipolar dendrites are present at P13 and P30 compared with line-5. It is difficult to treat the retinal degeneration if the disease progress is so fast that does not allow normal photoreceptor development. Based on this reason, it could be more appropriate to use line-5 for photoreceptor rescue therapy approaches. However, a recent study using *S334ter* line-3 found a good outer segment rescue effect in cones using CNTF (Li et al., 2010). On the other hand, cell replacement therapies in line-3 rats need to include other retinal cells besides photoreceptors for successful restoration of visual responses (Sagdullaev et al., 2003; Seiler et al., 2008a,b, 2010).

Appendix. Supplementary data

Supplementary data associated with this article can be found in the online version, at doi:10.1016/j.exer.2010.12.001.

References

An, G.J., Asayama, N., Humayun, M.S., Weiland, J., Cao, J., Kim, S.Y., Grebe, R., de Juan Jr., E., Sadda, S., 2002. Ganglion cell responses to retinal light stimulation in the absence of photoreceptor outer segments from retinal degenerate rodents. Curr. Eye Res. 24, 26–32.

Barhoum, R., Martinez-Navarrete, G., Corrochano, S., Germain, F., Fernandez-Sanchez, L., de la Rosa, E.J., de la Villa, P., Cuenca, N., 2008. Functional and structural modifications during retinal degeneration in the rd10 mouse. Neuroscience 155, 698–713.

Berger, W., Kloeckener-Gruissem, B., Neidhardt, J., 2010. The molecular basis of human retinal and vitreoretinal diseases. Prog. Retin. Eye Res. 29, 335–375.

Brandstatter, J.H., Fletcher, E.L., Garner, C.C., Gundelfinger, E.D., Wässle, H., 1999. Differential expression of the presynaptic cytomatrix protein bassoon among ribbon synapses in the mammalian retina. Eur. J. Neurosci. 11, 3683–3693.

Cuenca, N., Pinilla, I., Sauve, Y., Lu, B., Wang, S., Lund, R.D., 2004. Regressive and reactive changes in the connectivity patterns of rod and cone pathways of P23H transgenic rat retina. Neuroscience 127, 301–317.

Cuenca, N., Pinilla, I., Sauve, Y., Lund, R., 2005. Early changes in synaptic connectivity following progressive photoreceptor degeneration in RCS rats. Eur. J. Neurosci. 22, 1057–1072.

Dorfman, A.L., Cuenca, N., Pinilla, I., Joly, S., Chemtob, S., Lachapelle, P., 2006. Retinal cytoarchitectural anomalies following postnatal hyperoxia: more than what originally met the eye. Invest. Ophthalmol. Vis. Sci. 47 E-Abstract 3084.

Euler, T., Wässle, H., 1995. Immunocytochemical identification of cone bipolar cells in the rat retina. J. Comp. Neurol. 361, 461–478.

Green, E.S., Menz, M.D., LaVail, M.M., Flannery, J.G., 2000. Characterization of rhodopsin mis-sorting and constitutive activation in a transgenic rat model of retinitis pigmentosa. Invest. Ophthalmol. Vis. Sci. 41, 1546–1553.

Hombrebueno, J.R., Tsai, M.M., Kim, H.L., De Juan, J., Grzywacz, N.M., Lee, E.J., 2010. Morphological changes of short-wavelength cones in the developing S334ter-3 transgenic rat. Brain Res. 1321, 60–66.

Jensen, R.J., Rizzo 3rd, J.F., 2009. Activation of ganglion cells in wild-type and rd1 mouse retinas with monophasic and biphasic current pulses. J. Neural. Eng. 6 035004.

Johnson, J., Tian, N., Caywood, M.S., Reimer, R.J., Edwards, R.H., Copenhagen, D.R., 2003. Vesicular neurotransmitter transporter expression in developing post-natal rodent retina: GABA and glycine precede glutamate. J. Neurosci. 23, 518–529.

Jones, B.W., Marc, R.E., 2005. Retinal remodeling during retinal degeneration. Exp. Eye Res. 81, 123–137.

Jones, B.W., Watt, C.B., Frederick, J.M., Baehr, W., Chen, C.K., Levine, E.M., Milam, A.H., LaVail, M.M., Marc, R.E., 2003. Retinal remodeling triggered by photoreceptor degenerations. J. Comp. Neurol. 464, 1–16.

Kolb, H., Zhang, L., Dekorver, L., Cuenca, N., 2002. A new look at calretinin-immunoreactive amacrine cell types in the monkey retina. J. Comp. Neurol. 453, 168–184.

Kolomiets, B., Dubus, E., Simonutti, M., Rosolen, S., Sahel, J.A., Picaud, S., 2010. Late histological and functional changes in the P23H rat retina after photoreceptor loss. Neurobiol. Dis. 38, 47–58.

Lee, E.S., Flannery, J.G., 2007. Transport of truncated rhodopsin and its effects on rod function and degeneration. Invest. Ophthalmol. Vis. Sci. 48, 2868–2876.

Li, Y., Tao, W., Luo, L., Huang, D., Kauper, K., Stabila, P., LaVail, M.M., Laties, A.M., Wen, R., 2010. CNTF induces regeneration of cone outer segments in a rat model of retinal degeneration. PLoS ONE 5, e9495.

Lin, B., Masland, R.H., Strettoi, E., 2009. Remodeling of cone photoreceptor cells after rod degeneration in rd mice. Exp. Eye Res. 88, 589–599.

Lin, J.H., LaVail, M.M., 2010. Misfolded proteins and retinal dystrophies. Adv. Exp. Med. Biol. 664, 115–121.

Liu, C., Li, Y., Peng, M., Laties, A.M., Wen, R., 1999. Activation of caspase-3 in the retina of transgenic rats with the rhodopsin mutation s334ter during photoreceptor degeneration. J. Neurosci. 19, 4778–4785.

Marc, R.E., Jones, B.W., Anderson, J.R., Kinard, K., Marshak, D.W., Wilson, J.H., Wensel, T., Lucas, R.J., 2007. Neural reprogramming in retinal degeneration. Invest. Ophthalmol. Vis. Sci. 48, 3364–3371.

Marc, R.E., Jones, B.W., Watt, C.B., Strettoi, E., 2003. Neural remodeling in retinal degeneration. Prog. Retin. Eye Res. 22, 607–655.

Marc, R.E., Jones, B.W., Watt, C.B., Vazquez-Chona, F., Vaughan, D.K., Organisciak, D.T., 2008. Extreme retinal remodeling triggered by light damage: implications for age related macular degeneration. Mol. Vis. 14, 782–806.

Margolis, D.J., Newkirk, G., Euler, T., Detwiler, P.B., 2008. Functional stability of retinal ganglion cells after degeneration-induced changes in synaptic input. J. Neurosci. 28, 6526–6536.

Martinez-Navarrete, G., Seiler, M.J., Aramant, R.B., Pinilla, I., Cuenca, N., 2006. Outer retinal changes and apoptosis rate in S334ter and RCS rats. Invest. Ophthalmol. Vis. Sci. 46 ARVO E-abstract 5785.

Mazzoni, F., Novelli, E., Strettoi, E., 2008. Retinal ganglion cells survive and maintain normal dendritic morphology in a mouse model of inherited photoreceptor degeneration. J. Neurosci. 28, 14282–14292.

McGinnis, J.F., Stepanik, P.L., Jariangprasert, S., Lerious, V., 1997. Functional significance of recoverin localization in multiple retina cell types. J. Neurosci. Res. 50, 487–495.

Naash, M.I., Ripps, H., Li, S., Goto, Y., Peachey, N.S., 1996. Polygenic disease and retinitis pigmentosa: albinism exacerbates photoreceptor degeneration induced by the expression of a mutant opsin in transgenic mice. J. Neurosci. 16, 7853–7858.

Nagar, S., Krishnamoorthy, V., Cherukuri, P., Jain, V., Dhingra, N.K., 2009. Early remodeling in an inducible animal model of retinal degeneration. Neuroscience 160, 517–529.

Peng, Y.W., Senda, T., Hao, Y., Matsuno, K., Wong, F., 2003. Ectopic synaptogenesis during retinal degeneration in the Royal College of Surgeons rat. Neuroscience 119, 813–820.

Pennesi, M.E., Nishikawa, S., Matthes, M.T., Yasumura, D., LaVail, M.M., 2008. The relationship of photoreceptor degeneration to retinal vascular development and loss in mutant rhodopsin transgenic and RCS rats. Exp. Eye Res. 87, 561–570.

Pinilla, I., Cuenca, N., Martinez-Navarrete, G., Lund, R.D., Sauve, Y., 2009. Intraretinal processing following photoreceptor rescue by non-retinal cells. Vision Res. 49, 2067–2077.

Pinilla, I., Cuenca, N., Sauve, Y., Wang, S., Lund, R.D., 2007. Preservation of outer retina and its synaptic connectivity following subretinal injections of human RPE cells in the Royal College of Surgeons rat. Exp. Eye Res. 85, 381–392.

Ray, A., Sun, G.J., Chan, L., Grzywacz, N.M., Weiland, J., Lee, E.J., 2010. Morphological alterations in retinal neurons in the S334ter-line3 transgenic rat. Cell Tissue Res. 339, 481–491.

Rosenfeld, P.J., Cowley, G.S., McGee, T.L., Sandberg, M.A., Berson, E.L., Dryja, T.P., 1992. A null mutation in the rhodopsin gene causes rod photoreceptor dysfunction and autosomal recessive retinitis pigmentosa. Nat. Genet. 1, 209–213.

Sagdullaev, B.T., Aramant, R.B., Seiler, M.J., Woch, G., McCall, M.A., 2003. Retinal transplantation-induced recovery of retinotectal visual function in a rodent model of retinitis pigmentosa. Invest. Ophthalmol. Vis. Sci. 44, 1686–1695.

Seiler, M.J., Aramant, R.B., Thomas, B.B., Peng, Q., Sadda, S.R., Keirstead, H.S., 2010. Visual restoration and transplant connectivity in degenerate rats implanted with retinal progenitor sheets. Eur. J. Neurosci. 31, 508–520.

Seiler, M.J., Thomas, B.B., Chen, Z., Arai, S., Chadalavada, S., Mahoney, M.J., Sadda, S.R., Aramant, R.B., 2008a. BDNF-treated retinal progenitor sheets transplanted to degenerate rats: improved restoration of visual function. Exp. Eye Res. 86, 92–104.

Seiler, M.J., Thomas, B.B., Chen, Z.R.W., Sadda, S.R., Aramant, R.B., 2008b. Retinal transplants restore visual responses − trans-synaptic tracing from visually responsive sites labels transplant neurons. Eur. J. Neurosci. 28, 208–220.

Shastry, B.S., 1994. Retinitis pigmentosa and related disorders: phenotypes of rhodopsin and peripherin/RDS mutations. Am. J. Med. Genet. 52, 467–474.

Sohocki, M.M., Daiger, S.P., Bowne, S.J., Rodriquez, J.A., Northrup, H., Heckenlively, J.R., Birch, D.G., Mintz-Hittner, H., Ruiz, R.S., Lewis, R.A., Saperstein, D.A., Sullivan, L.S., 2001. Prevalence of mutations causing retinitis pigmentosa and other inherited retinopathies. Hum. Mutat. 17, 42–51.

Steinberg, R.H., Flannery, J.G., Naash, M., Oh, P., Matthes, M.T., Yasumura, D., Lau-Villacorta, C., Chen, J., LaVail, M.M., 1996. Transgenic rat models of inherited retinal degeneration caused by mutant opsin genes [ARVO abstract]. Invest. Ophthalmol. Vis. Sci. 37, S698.

Strettoi, E., Mears, A.J., Swaroop, A., 2004. Recruitment of the rod pathway by cones in the absence of rods. J. Neurosci. 24, 7576–7582.

Strettoi, E., Pignatelli, V., Rossi, C., Porciatti, V., Falsini, B., 2003. Remodeling of second-order neurons in the retina of rd/rd mutant mice. Vision Res. 43, 867–877.

Sullivan, R., Penfold, P., Pow, D.V., 2003. Neuronal migration and glial remodeling in degenerating retinas of aged rats and in nonneovascular AMD. Invest. Ophthalmol. Vis. Sci. 44, 856–865.

Thomas, B.B., Seiler, M.J., Sadda, S.R., Aramant, R.B., 2004. Superior colliculus responses to light − preserved by transplantation in a slow degeneration rat model. Exp. Eye Res. 79, 29–39.

Voigt, T., Wässle, H., 1987. Dopaminergic innervation of A II amacrine cells in mammalian retina. J. Neurosci. 7, 4115–4128.

Wang, D.Y., Chan, W.M., Tam, P.O., Baum, L., Lam, D.S., Chong, K.K., Fan, B.J., Pang, C.P., 2005. Gene mutations in retinitis pigmentosa and their clinical implications. Clin. Chim. Acta 351, 5–16.

Wang, Q., Chen, Q., Zhao, K., Wang, L., Traboulsi, E.I., 2001. Update on the molecular genetics of retinitis pigmentosa. Ophthal. Genet. 22, 133–154.

Wässle, H., Grunert, U., Rohrenbeck, J., 1993. Immunocytochemical staining of AII-amacrine cells in the rat retina with antibodies against parvalbumin. J. Comp. Neurol. 332, 407–420.

Zhang, H., Huang, W., Zhu, X., Craft, C.M., Baehr, W., Chen, C.K., 2003. Light-dependent redistribution of visual arrestins and transducin subunits in mice with defective phototransduction. Mol. Vis. 9, 231–237.